Probing Quantum Commutation Rules by Addition and Subtraction of Single Photons to/from a Light Field

Valentina Parigi, *et al.*

Science **317**, 1890 (2007);
DOI: 10.1126/science.1146204

The Voyager profiles (Fig. 4, B and C) look very different from ours, but a few features clearly correspond to known rings. Stellar occultations have revealed that two uranian rings have broad, optically thin components (*17*): Ring η has a 55-km outward extension and ring δ has a 12-km inward extension. The η ring's extension provides a natural explanation for its rapid growth in brightness as *B* decreases. Furthermore, Fig. 4C shows a subtle inflection closely aligned with ring δ, suggesting that its optically thin companion is glowing brighter at small *B*. Ring λ illustrates how a dusty ring should appear in our data (Fig. 4C). It is visible but at a level about 150 times as faint as that in the high-phase Voyager image. Such a ratio is compatible with the typical light-scattering properties of micron-sized dust. A broad feature at 43,000 km (from the center of Uranus) could also be related to dust seen by Voyager, but this feature remains somewhat ambiguous in our data because it was only detected on the south ansa (Fig. 2).

Many of the other ring components are difficult to reconcile with known rings. If such features are long-term members of the system, then they somehow escaped detection. Consider the region near 45,000 km, which is nearly devoid of dust according to Voyager but is about half as bright as the η ring in our profile. One can devise an optically thin, backscattering population that fits the data, but extensive imaging by Voyager revealed no such population.

Even stranger is the ζ ring, which shifted radially from the Voyager epoch to the present. Because of the different phase angles, one cannot make any conclusive inferences about the particle sizes. Nevertheless, we require a broad, backscattering population centered at 40,000 km from the center of Uranus and an overlapping, slightly less backscattering population shifted inward by several thousand kilometers. Such an explanation seems rather ad hoc, and it is difficult to understand how particles of slightly different sizes and scattering properties could become spatially segregated.

A simpler alternative is that the faint material we see is indeed dust but that its radial distribution has changed since 1986, in fact much more dramatically than was suggested a year ago (*7*). One usually assumes that ring systems are static, but we now have several counterexamples. At Saturn, the D ring has changed substantially from the Voyager epoch (1980–1981) to the present (*18*), and the F ring also shows numerous changes (*19*). At Neptune, the pattern of dusty arcs in the Adams ring is very different now as compared with that from Voyager's first images in 1989 (*20*, *21*). We conclude that changes in dusty rings over ~20-year time scales are common. The changes seen in Uranus' ring system, however, are much larger in scale than anything seen previously.

Changes over year-to-decade time scales are dynamically plausible because the dust populations that we see represent extremely tiny amounts of material, and the orbits of small dust grains evolve rapidly in response to nongravitational forces (e.g., Poynting-Robertson and plasma drag, Lorentz forces) (*22*). The rings were once expected to represent a steady state between dust creation and removal processes. However, we now realize that these states are far from steady and may be dominated by infrequent events, such as large impacts, that inject highly visible quantities of dust, as has been discussed for Saturn's A ring (*23*).

References and Notes

1. B. A. Smith *et al.*, *Science* **233**, 43 (1986).
2. J. L. Elliot, E. W. Dunham, D. J. Mink, *Nature* **267**, 328 (1977).
3. P. D. Nicholson *et al.*, *Science* **272**, 509 (1996).
4. G. Verbanac, I. de Pater, M. R. Showalter, J. J. Lissauer, *Icarus* **174**, 241 (2005).
5. I. de Pater, S. Martin, M. R. Showalter, *Icarus* **172**, 446 (2004).
6. Materials and methods are available as supporting material on *Science* Online.
7. I. de Pater, S. G. Gibbard, H. B. Hammel, *Icarus* **180**, 186 (2006).
8. M. R. Showalter, J. J. Lissauer, *Science* **311**, 973 (2006).
9. I. de Pater, H. B. Hammel, S. G. Gibbard, M. R. Showalter, *Science* **312**, 92 (2006).
10. S. G. Gibbard, I. de Pater, H. B. Hammel, *Icarus* **174**, 253 (2005).
11. I. de Pater *et al.*, *Icarus* **160**, 359 (2002).
12. K. Matthews, G. Neugebauer, P. D. Nicholson, *Icarus* **52**, 126 (1982).
13. E. Karkoschka, *Icarus* **151**, 51 (2001).
14. The International Astronomical Union definition of the ζ ring identifies the ring with R/1986 U 2 but uses the location and extent of the ζ ring as determined in (*7*); see (http://planetarynames.wr.usgs.gov/append8.html).
15. M. R. Showalter, J. A. Burns, J. N. Cuzzi, *Icarus* **69**, 458 (1987).
16. I. de Pater *et al.*, *Icarus* **138**, 214 (1999).
17. R. G. French, P. D. Nicholson, C. C. Porco, E. A. Marouf, in *Uranus*, J. T. Bergstrahl, E. D. Miner, M. S. Matthews, Eds. (Univ. of Arizona Press, Tucson, AZ, 1991), pp. 317–409.
18. M. M. Hedman *et al.*, *Icarus* **188**, 89 (2007).
19. M. R. Showalter, *Icarus* **171**, 356 (2004).
20. C. Dumas, R. J. Terrile, B. A. Smith, G. Schneider, E. E. Becklin, *Nature* **400**, 733 (1999).
21. I. de Pater *et al.*, *Icarus* **174**, 263 (2005).
22. J. A. Burns *et al.*, in *Jupiter: The Planet, Satellites and Magnetosphere*, F. Bagenal, T. E. Dowling, W. B. McKinnon, Eds. (Cambridge Univ. Press, Cambridge, 2004), pp. 241–262.
23. L. W. Esposito *et al.*, *Science* **307**, 1251 (2005).

24. We thank E. M. Johansson, P. J. Stomski Jr., R. J. Sumner, J. C. Y. Chin, and P. L. Wizinowich at the W. M. Keck Observatory for upgrading the AO system. This work was funded by NSF and the Technology Center for Adaptive Optics, managed by the University of California at Santa Cruz under cooperative agreement no. AST-9876783. The W. M. Keck Observatory is operated as a scientific partnership among the California Institute of Technology, the University of California, and the National Aeronautics and Space Administration (NASA), and was built with financial support of the W. M. Keck Foundation. Further support was provided by NASA grants NNX07AK70G (I.d.P.), NNX06AD12G and NNG06GI25G (H.B.H.), and NNX06AB98G (M.R.S.).

Supporting Online Material

www.sciencemag.org/cgi/content/full/1148103/DC1
Materials and Methods
Fig. S1
References

20 July 2007; accepted 16 August 2007
Published online 23 August 2007;
10.1126/science.1148103
Include this information when citing this paper.

Probing Quantum Commutation Rules by Addition and Subtraction of Single Photons to/from a Light Field

Valentina Parigi,[1] Alessandro Zavatta,[2] Myungshik Kim,[3] Marco Bellini[1,4]*

The possibility of arbitrarily "adding" and "subtracting" single photons to and from a light field may give access to a complete engineering of quantum states and to fundamental quantum phenomena. We experimentally implemented simple alternated sequences of photon creation and annihilation on a thermal field and used quantum tomography to verify the peculiar character of the resulting light states. In particular, as the final states depend on the order in which the two actions are performed, we directly observed the noncommutativity of the creation and annihilation operators, one of the cardinal concepts of quantum mechanics, at the basis of the quantum behavior of light. These results represent a step toward the full quantum control of a field and may provide new resources for quantum information protocols.

Classically, the operation of deterministically adding an object to an ensemble and then subtracting another leaves the statistics unaltered, as long as all the objects are identical. The probability distribution would just shift by one unit toward larger values when one object is added and then shift back to its initial position when another is extracted. For an ensemble of identical quantum particles, however, the situation may be different. For example, if the particles were photons in a single-mode radiation field, one would naturally use the bosonic creation and annihilation operators $\hat{a}^{\dagger}$ and $\hat{a}$ to perform the addition and the subtraction of single photons to and from the light field. Indeed, for the general case of a quantum light field described by

a density matrix $\hat{\rho}$, there is a broad consensus in calling the result of the application of the creation (annihilation) operator, $\hat{a}^\dagger\hat{\rho}\hat{a}$ ($\hat{a}\hat{\rho}\hat{a}^\dagger$), the "photon-added" ("-subtracted") state, after proper normalization. This tendency derives from the fact that, when the photon creation operator $\hat{a}^\dagger$ acts on a state with a well-defined number n of photons (also called a Fock or number state, and denoted by $|n\rangle$), it increases this number by one:

$$\hat{a}^\dagger|n\rangle = \sqrt{n+1}|n+1\rangle. \quad (1)$$

Conversely, when the photon annihilation operator $\hat{a}$ acts on the same state, it subtracts a quantum of excitation, thus reducing the number of photons in the state by exactly one (*1*, *2*):

$$\hat{a}|n\rangle = \sqrt{n}|n-1\rangle. \quad (2)$$

When the initial number of particles is precisely known, the quantum and the classical cases give exactly the same results for arbitrary sequences of additions and subtractions. However, the situation changes completely for general superpositions or mixtures of Fock states. After the operation of particle subtraction, the average number of quantum particles in certain states may unexpectedly grow instead of diminishing, as one would be naturally tempted to expect (*2*). Furthermore, adding one particle to the system by a creation operator and then, immediately after, subtracting another by an annihilation operator would lead to a final probability distribution of the ensemble completely different from the initial one. Although counterintuitive, this behavior is not unphysical and does not put energy conservation at stake: It simply derives from the misleading implicit assumption that a deterministic addition and subtraction of particles can be represented by the creation and annihilation operators which, on the contrary, work in a probabilistic way.

For light, it is straightforward to show that the operation of photon addition always produces a nonclassical light state (*3*–*6*), whereas photon subtraction gives a final nonclassical field only if the original one was already nonclassical (*7*, *8*). Apart from the particular case of Fock states, and in an apparent contrast to the classical situation, the sequence of photon creation and annihilation always creates a state different from the original one. Furthermore, due to the noncommutativity of $\hat{a}^\dagger$ and $\hat{a}$ (i.e., $[\hat{a},\hat{a}^\dagger] \neq 0$), the reverse sequence of operators is expected to produce another state that is different from both, as $\hat{a}\hat{a}^\dagger \neq \hat{a}^\dagger\hat{a} \neq \mathbf{1}$.

A thermal state is the most classical state of light, formed by a statistical mixture of coherent states. Its density matrix is diagonal in the Fock state basis and, accordingly, exhibits no phase dependence. It can thus be completely described in terms of its photon number distribution. The addition and subtraction of a single photon from the spatiotemporal mode containing the thermal light state can be performed in a conditional way, that is, by producing the target photon-added or -subtracted state only upon the positive outcome of a separate measurement. In particular, the controlled addition of a single photon can be realized by the conditional stimulated parametric down-conversion in a nonlinear optical crystal (*3*–*5*). When an ultraviolet pump photon interacts in the crystal, it may spontaneously decay into two quantum-mechanically entangled infrared (IR) photons traveling along different directions (conserving the total momentum) and with energies that sum up to that of the parent photon. When one of the two IR photons (the so-called trigger photon) is detected along a particular direction with a given energy, the spatial properties and the energy of the other are also unambiguously determined. If one injects a seed light field into the crystal, then stimulated emission may occur into the same mode, and the detection of the trigger photon now indicates the conditional generation of the photon-added seed state in a well-defined spatiotemporal mode.

The implementation of photon subtraction implies the controlled reflection of a single photon off the right mode by a beam splitter (*7*). A "click" in an on/off photodetector placed in the reflected path indicates the successful subtraction of a single photon from the input field. It can be explicitly proven that the above procedures for conditional single-photon addition and subtraction from a light field are faithful implementations of the photon creation and annihilation operators $\hat{a}^\dagger$ and $\hat{a}$ for sufficiently low crystal parametric gain and beam-splitter reflectivity (*2*). Combining single-photon addition and subtraction by such methods constitutes a much harder experimental challenge because it requires a perfect matching of all the involved field modes and implies a double conditioning, with a much lower success rate, to prepare the final light state.

To perform the two operations in two separate sequences, we have combined three different modules, each implementing the action of a specific

[1]European Laboratory for Nonlinear Spectroscopy (LENS), Via Nello Carrara 1, 50019 Sesto Fiorentino, Florence, Italy. [2]Department of Physics, University of Florence, I-50019 Sesto Fiorentino, Florence, Italy. [3]School of Mathematics and Physics, The Queen's University, Belfast, BT7 1NN, UK. [4]Istituto Nazionale di Ottica Applicata (CNR), Largo E. Fermi, 6, I-50125, Florence, Italy.
*To whom correspondence should be addressed. E-mail: bellini@inoa.it

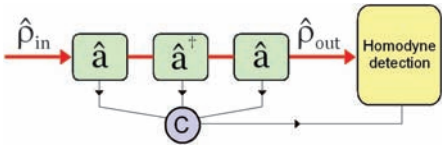

Fig. 1. Schematic of the sequence of modules representing specific quantum operators acting on a quantum light field (denoted by its density matrix $\hat{\rho}_{in}$). A module for single-photon creation (denoted by $\hat{a}^\dagger$) is placed between two modules for single-photon annihilation (denoted by $\hat{a}$). The final state $\hat{\rho}_{out}$ is conditionally prepared and analyzed by the homodyne detector whenever a specific sequence of "clicks" arrives from the modules and is passed on by the logic circuit (C). Single-click events herald the production of a "photon-added" or "photon-subtracted" state. Double-click events herald the production of a quantum state that has undergone the sequence of photon addition and subtraction or vice versa. Double photon-subtraction events are not considered in the present experiment.

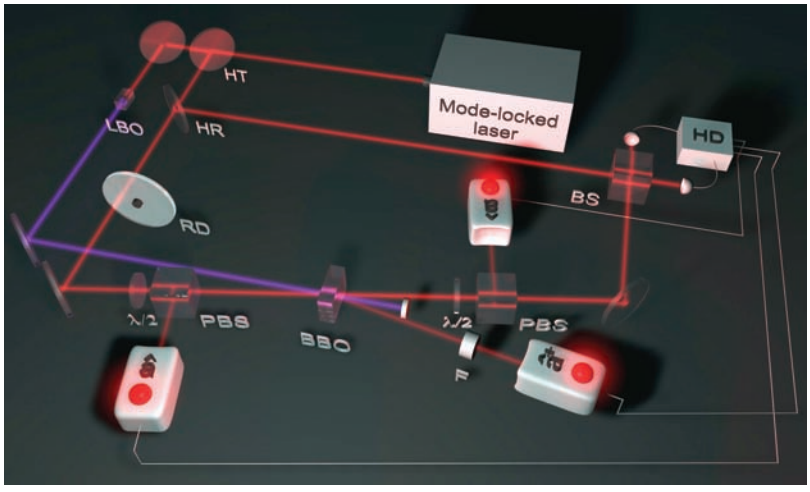

Fig. 2. Experimental setup. Pulses at a wavelength of 786 nm are emitted at a repetition rate of 82 MHz from a mode-locked picosecond Ti:sapphire laser. They are split by a high-transmission (HT) and a high-reflectivity (HR) beam splitter to serve as (i) the pump for parametric down-conversion in a 3-mm-thick, type-I beta-barium borate (BBO) crystal after frequency-doubling in a lithium triborate (LBO) crystal; (ii) the seed thermal field, after scattering off a rotating ground glass disk (RD) and spatial cleaning by a single-mode optical fiber (not shown); and (iii) the local oscillator field for balanced homodyne detection (HD) after mixing with the investigated states in a 50% beam splitter (BS). F is a combination of spectral and spatial filters made of a pair of etalon interference filters with a narrow (50 GHz) spectral width, and a single-mode optical fiber directly connected to an on/off photodetector (Perkin-Elmer SPCM AQR-14, denoted by $\hat{a}^\dagger$). Pairs of half-wave plates ($\lambda/2$) and polarizing beam splitters (PBS) serve to implement the photon-subtraction modules together with fiber-coupled on/off photodetectors (denoted by $\hat{a}$).

quantum operator on the light state (Fig. 1). Two combinations of half-wave plates and polarizing beam splitters, together with on/off photodetectors in the reflected channel, form the photon-subtraction modules that are placed in the path of the thermal light field, respectively before and after the parametric crystal that, with the on/off photodetector in the trigger channel, forms the photon-addition module. By rotating the two half-wave plates, we can control the beam-splitter reflectivities to alternately switch off one or both of the subtraction modules. Then, by choosing the right combination of clicks coming from the module detectors, we can select the desired quantum operation, or any sequence of them. A single click simply conditions the generation of a photon-added or photon-subtracted thermal state, whereas a double click can either produce a first-subtracted-then-added thermal state or vice versa, depending on the combination of clicks. We use a synchronized, ultrafast, time-domain, balanced homodyne detector (*9*) to analyze the conditionally prepared states by repeatedly measuring their electric field quadratures and building up quadrature distributions. The reference field (usually named "local oscillator") for the homodyne measurements comes from the same picosecond pulsed laser, which provides the thermal seed field and, once frequency-doubled, the pump pulses for the parametric crystal (Fig. 2). As the generated states are, by construction, phase independent, we have acquired about 10^5 quadrature measurements per state, leaving the phase of the local oscillator unlocked. As the combined action of addition and subtraction is rather rare (with only about 10 double-click events every second), a full quadrature distribution may take up to 5 hours to acquire in such cases.

We have first measured the unperturbed thermal light field, then the state resulting from single-photon addition, single-photon subtraction, and from both the addition-subtraction and subtraction-addition sequences. Figure 3 shows the experimental quadrature distributions for all the states obtained from an initial thermal distribution with $\bar{n} = 0.57$, together with the curves calculated while keeping all experimental inefficiencies into account (*2*). Next to them, the corresponding photon number probability distributions are plotted as theoretically calculated and as reconstructed from the experimental data by means of an iterative maximum likelihood algorithm (*10*–*12*), correcting for the finite detection efficiency (*2*).

The first interesting result appears when comparing the mean photon numbers of the states: For the photon-added state one finds, quite naturally, that the mean photon number is larger than in the original thermal light state, but unexpectedly the same result occurs for the photon-subtracted state. The operation of removing one photon from the field has increased (doubled) its final mean photon number. Such an increase also takes place for the sequence of operators that should intuitively bring the field back to the initial state.

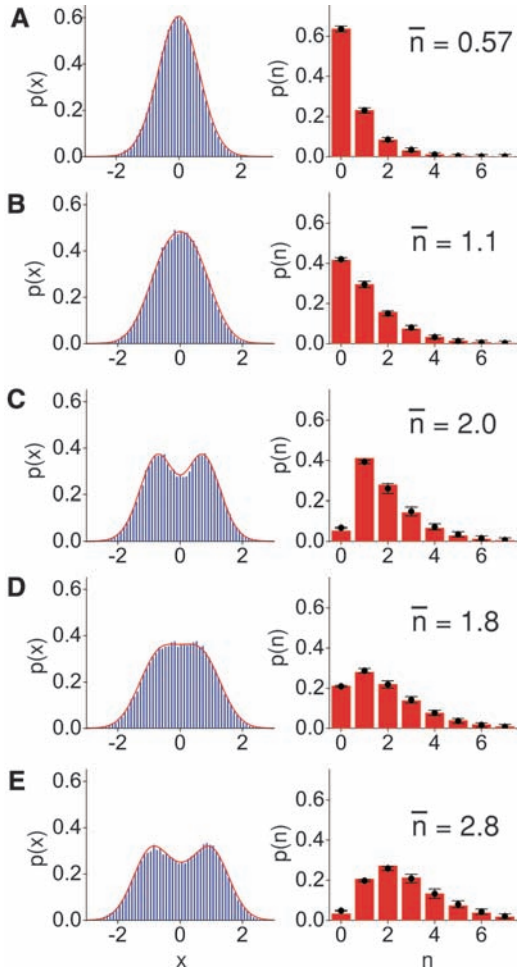

Fig. 3. Experimental quadrature distribution histograms and theoretical curves (superposed solid lines) for (**A**) the original thermal state; (**B**) the photon-subtracted state; (**C**) the photon-added state; (**D**) the photon-added-then-subtracted state; (**E**) the photon-subtracted-then-added state. The second column shows the corresponding theoretical (red bars) and experimentally reconstructed (solid circles with error bars) photon number distributions. States resulting from a final photon addition present a very small vacuum contribution, which makes them highly nonclassical. The residual vacuum term derives from imperfections in the preparation of the states and is satisfactorily accounted for by the theoretical model (*2*). The mean photon number in the state is also shown as calculated from the reconstructed distributions.

The experimentally reconstructed density matrix elements for the states have then been used to obtain their corresponding Wigner functions (WFs) (*13*). Quasi-probability distributions fully describe the state of a quantum system in phase-space (the space spanned by two orthogonal quadratures of the electromagnetic field for a single-mode state of light, as in this case) in the same manner as a positive-definite probability distribution characterizes a classical system. The negativity of the WF is indeed a good indication of the highly nonclassical character of the state.

A clear negativity of the reconstructed WFs (which survives even without correcting for detection losses) is obtained in all the cases where photon addition is the last operator acting on the states, thus showing their high degree of nonclassicality. However, the WFs of states resulting from the two sequences of addition and subtraction show other interesting features (Fig. 4). The two final states are different from each other and from the original thermal state. In both cases, the WF exhibits a clear central dip, which is absent in the WF of the thermal field; such a dip reaches negative values for the subtract-then-add sequence, whereas it stays well in the positive region for the add-then-subtract sequence (*14*). This provides a direct experimental verification of the noncommutativity of the quantum bosonic creation and annihilation operators and gives a visually convincing demonstration that a simple view of classical particle addition and subtraction is incorrect in this case. The noncommutativity of bosonic annihilation and creation operators is at the basis of many "weird" quantum phenomena of light. The mere existence of a vacuum field (with spontaneous emission, the Lamb shift, or the Casimir effect as some of its main manifestations) is a direct consequence of this. Furthermore, the difference in the resulting states obtained by applying noncommuting quantum operators in re-

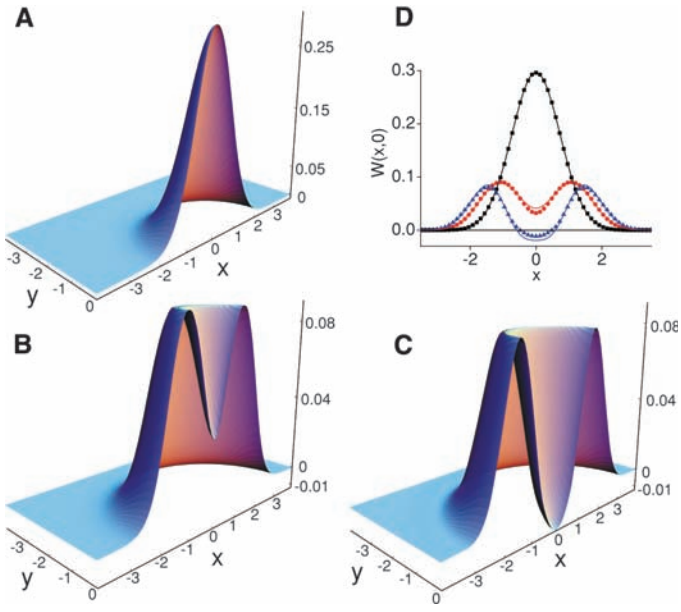

Fig. 4. Experimental WFs (corrected for detection inefficiency) for (**A**) the original thermal state; (**B**) the photon-added-then-subtracted state; (**C**) the photon-subtracted-then-added state. (**D**) presents sections of the above Wigner functions (black squares correspond to the thermal field; red circles and blue triangles correspond to the photon-added-then-subtracted and the photon-subtracted-then-added states, respectively), together with the corresponding theoretical predictions (solid curves) (*2*).

verse order, as in this case, is the real essence of the Heisenberg uncertainty principle. Besides its fundamental importance, the experimental implementation of such a sequence of basic quantum operations is an essential tool for the full-scale engineering of a quantum light state optimized for a multitude of different tasks (*15*), including robust quantum communication. As any quantum operation, including non-Gaussian operations, is composed of photon additions and subtractions (i.e, it can be expressed as $f(\hat{a},\hat{a}^{\dagger})$), our experimental results constitute a step toward the full quantum control of a field and the generation of highly entangled states (*16*).

References and Notes

1. P. A. M. Dirac, *The Principles of Quantum Mechanics* (Oxford Press, 1954).
2. Materials and methods are available as supporting material on *Science* Online.
3. A. Zavatta, S. Viciani, M. Bellini, *Science* **306**, 660 (2004).
4. A. Zavatta, S. Viciani, M. Bellini, *Phys. Rev. A* **72**, 023820 (2005).
5. A. Zavatta, V. Parigi, M. Bellini, *Phys. Rev. A* **75**, 052106 (2007).
6. C. T. Lee, *Phys. Rev. A* **52**, 3374 (1995).
7. J. Wenger, R. Tualle-Brouri, P. Grangier, *Phys. Rev. Lett.* **92**, 153601 (2004).
8. M. S. Kim, E. Park, P. L. Knight, H. Jeong, *Phys. Rev. A* **71**, 043805 (2005).
9. A. Zavatta, M. Bellini, P. L. Ramazza, F. Marin, F. T. Arecchi, *J. Opt. Soc. Am. B* **19**, 1189 (2002).
10. K. Banaszek, G. M. D'Ariano, M. G. A. Paris, M. F. Sacchi, *Phys. Rev. A* **61**, 010304(R) (1999).
11. A. I. Lvovsky, *J. Opt. B: Quantum Semiclassical Opt.* **6**, S556 (2004).
12. Z. Hradil, D. Mogilevtsev, J. Rehacek, *Phys. Rev. Lett.* **96**, 230401 (2006).
13. U. Leonhardt, *Measuring the Quantum State of Light* (Cambridge University Press, Cambridge, 1997).
14. Note that the positivity of the WF in the case of the add-then-subtract sequence is not due to experimental imperfections. As for squeezed states, the resulting state can be shown to be nonclassical (with a negative P function), although possessing a positive WF.
15. F. Dell'Anno, S. De Siena, F. Illuminati, *Phys. Rep.* **428**, 53 (2006).
16. J. Eisert, S. Scheel, M. B. Plenio, *Phys. Rev. Lett.* **89**, 137903 (2002).

17. We thank F. T. Arecchi, A. Montina, and E. Park for helpful comments and for a critical reading of the manuscript, and P. Poggi for the improvement of detection electronics. This work was partially supported by Ente Cassa di Risparmio di Firenze and by the Italian Ministry of University and Scientific Research, under the PRIN 2005 initiative. M.S.K. acknowledges financial support from the UK Engineering and Physical Science Research Council (EPSRC) and Quantum Information Processing Interdisciplinary Research Centre (QIPIRC).

Supporting Online Material

www.sciencemag.org/cgi/content/full/317/5846/1890/DC1
Materials and Methods
References and Notes

7 June 2007; accepted 10 August 2007
10.1126/science.1146204

Symmetrized Characterization of Noisy Quantum Processes

Joseph Emerson,[1,2] Marcus Silva,[2,3] Osama Moussa,[2,3] Colm Ryan,[2,3] Martin Laforest,[2,3] Jonathan Baugh,[2] David G. Cory,[4] Raymond Laflamme[2,3,5]

A major goal of developing high-precision control of many-body quantum systems is to realize their potential as quantum computers. A substantial obstacle to this is the extreme fragility of quantum systems to "decoherence" from environmental noise and other control limitations. Although quantum computation is possible if the noise affecting the quantum system satisfies certain conditions, existing methods for noise characterization are intractable for present multibody systems. We introduce a technique based on symmetrization that enables direct experimental measurement of some key properties of the decoherence affecting a quantum system. Our method reduces the number of experiments required from exponential to polynomial in the number of subsystems. The technique is demonstrated for the optimization of control over nuclear spins in the solid state.

Quantum information enables efficient solutions to certain tasks that have no known efficient solution in the classical world, and it has reshaped our understanding of computational complexity. Harnessing the advantages of the quantum world requires the ability to robustly control quantum systems and, in particular, counteract the noise and decoherence affecting any physical realization of quantum information processors (QIPs). A pivotal step in this direction came with the discovery of quantum error correction codes (QECCs) (*1*, *2*) and the threshold theorem for fault-tolerant (FT) quantum computation (*3*–*6*). To make use of quantum error correction and produce fault-tolerant protocols, we need to understand the nature of the noise affecting the system at hand. There is a direct way to fully characterize the noise using a procedure known as process tomography (*7*–*9*). However, this procedure requires resources that grow exponentially with the number of subsystems (usually two-level systems called "qubits") and is intractable for characterizing the multi-qubit quantum systems that are presently realized

[1]Department of Applied Math, University of Waterloo, Waterloo, ON N2L 3G1, Canada. [2]Institute for Quantum Computing, University of Waterloo, Waterloo, ON N2L 3G1, Canada. [3]Department of Physics and Astronomy, University of Waterloo, Waterloo, ON N2L 3G1, Canada. [4]Department of Nuclear Science and Engineering, Massachusetts Institute of Technology, Cambridge, MA 02139, USA. [5]Perimeter Institute for Theoretical Physics, Waterloo, ON N2L 2Y5, Canada.